Anthracycline cardiotoxicity: role of metabolic vulnerability induced by cardiac pressure overload

Carlos Galán-Arriola, Daniel Pérez-Camargo, Inmaculada Jorge, Víctor Bautista, Ali Ayaon-Albarrán, Claudia Pérez-Martínez, Antonio de Molina-Iracheta, Laura Cádiz, Danielle Medina-Hernández, Carlos Caballero-Henares, Gonzalo J Lopez-Martín, Jesús Vázquez, Julien Ochala, Valentin Fuster, Javier Sánchez-González, Borja Ibáñez

ESC European Society of Cardiology

European Heart Journal (2026) **00**, 1–13
https://doi.org/10.1093/eurheartj/ehaf1060

TRANSLATIONAL SCIENCE
Cardio-oncology

Anthracycline cardiotoxicity: role of metabolic vulnerability induced by cardiac pressure overload

Carlos Galán-Arriola [1,2], Daniel Pérez-Camargo [3], Inmaculada Jorge [1,2], Víctor Bautista[4], Ali Ayaon-Albarrán[5], Claudia Pérez-Martínez[6], Antonio de Molina-Iracheta[1], Laura Cádiz[1], Danielle Medina-Hernández[1], Carlos Caballero-Henares[1], Gonzalo J. Lopez-Martín[1], Jesús Vázquez[1,2], Julien Ochala[7], Valentin Fuster [1,8], Javier Sánchez-González [9], and Borja Ibáñez [1,2,10,*]

[1]Centro Nacional de Investigaciones Cardiovasculares Carlos III (CNIC). c/Melchor Fernández Almagro, 3, Madrid 28029, Spain; [2]Centro de Investigación Biomédica en Red en Enfermedades Cardiovasculares (CIBERCV), Madrid, Spain; [3]Cardiac Surgery Department, Hospital Clínico San Carlos, Madrid, Spain; [4]Department of Surgery, Baylor College of Medicine at Christus Children's (Christus Health Santa Rosa), Houston, TX, USA; [5]Cardiac Surgery Department, Hospital la Paz, Madrid, Spain; [6]Facultad de Veterinaria, León University, León, Spain; [7]Department of Biomedical Sciences, University of Copenhagen, Copenhagen, Denmark; [8]Cardiology Department, Mount Sinai Fuster Heart Hospital, New York, NY, USA; [9]Philips Healthcare, Spain; and [10]Cardiology Department, Instituto de Investigación Sanitaria Fundación Jiménez Díaz (IIS-FJD, UAM), Madrid, Spain

Received 25 January 2025; revised 22 June 2025; accepted 11 December 2025

Abstract

Background and Aims Hypertension and valvular heart disease, both associated with left ventricular (LV) pressure overload, increase the risk of anthracycline cardiotoxicity. While epidemiologically established, the underlying mechanisms remain unclear, precluding identification of therapeutic targets.

Methods Two-month-old Yucatan pigs (males and females) underwent aortic banding to induce LV pressure overload or no operation. After 4 months, animals received a low-risk cumulative dose of doxorubicin (5 weekly 1 mg/kg intravenous injections) or vehicle, generating four groups: (i) healthy controls (no LV overload, no doxorubicin), (ii) Dox (doxorubicin, no LV overload), (iii) Banding (B: LV overload, no doxorubicin), and (iv) B + Dox (LV overload plus doxorubicin). Cardiac function, structure, and metabolism were assessed over 8 months by cardiac magnetic resonance, magnetic resonance spectroscopy, and hybrid positron emission tomography/computed tomography. At study end, proteomics and mitochondrial structure and function were analysed. Complementary *in vivo* and *ex vivo* studies examined the mechanistic role of energetic imbalance.

Results LV overload increased LV mass ($P < .0001$) and ejection fraction ($P = .0081$), with compensatory metabolic changes (drop in phosphocreatine ($P = .022$)). Low-risk Dox alone altered myocardial metabolism (increased glucose uptake, $P = .014$) but preserved cardiac function. In pigs with pre-existing LV pressure overload, doxorubicin increased mortality ($P < .0001$ vs all other groups), reduced left ventricular ejection fraction (LVEF) ($P < .0001$), increased fibrosis, and impaired mitochondrial respiration ($P = .032$). In HL-1 cardiomyocytes, reducing energy demand with mavacamten rescued cell viability under combined doxorubicin and hypertrophic stress.

Conclusions LV pressure overload increases myocardial susceptibility to anthracycline cardiotoxicity by inducing a high-energy-demand state. Anthracycline treatment, even at a low-risk dose, disrupts compensatory mechanisms in the pressure-overloaded heart, rapidly leading to cardiac dysfunction and heart failure. Preventive strategies targeting this metabolic vulnerability are urgently needed for patients with extant LV pressure overload (e.g. hypertension or valvular heart disease) who are undergoing anthracycline therapy.

* Corresponding author. Tel: +3491 4531200 (ext 4302), Email: bibanez@cnic.es

Structured Graphical Abstract

Key Question

Does pre-existing left ventricular (LV) pressure overload exacerbate anthracycline cardiotoxicity? What is the underlying mechanism linking pressure overload to increased susceptibility?

Key Finding

In Yucatan minipigs, LV pressure overload induced a hypermetabolic cardiac state with preserved function but reduced energetic reserve. In this setting, low-dose doxorubicin triggered severe mitochondrial dysfunction, myocardial fibrosis, and reduced survival. Reduction of energy demand by mavacamten was protective, confirming that energy mismatch was the cause of myocardial dysfunction.

Take Home Message

Pharmacological reduction of myocardial energy by mavacamten attenuates anthracycline-associated injury in subjects with pre-existing LV pressure overload (e.g. hypertension), supporting its utilization in this setting.

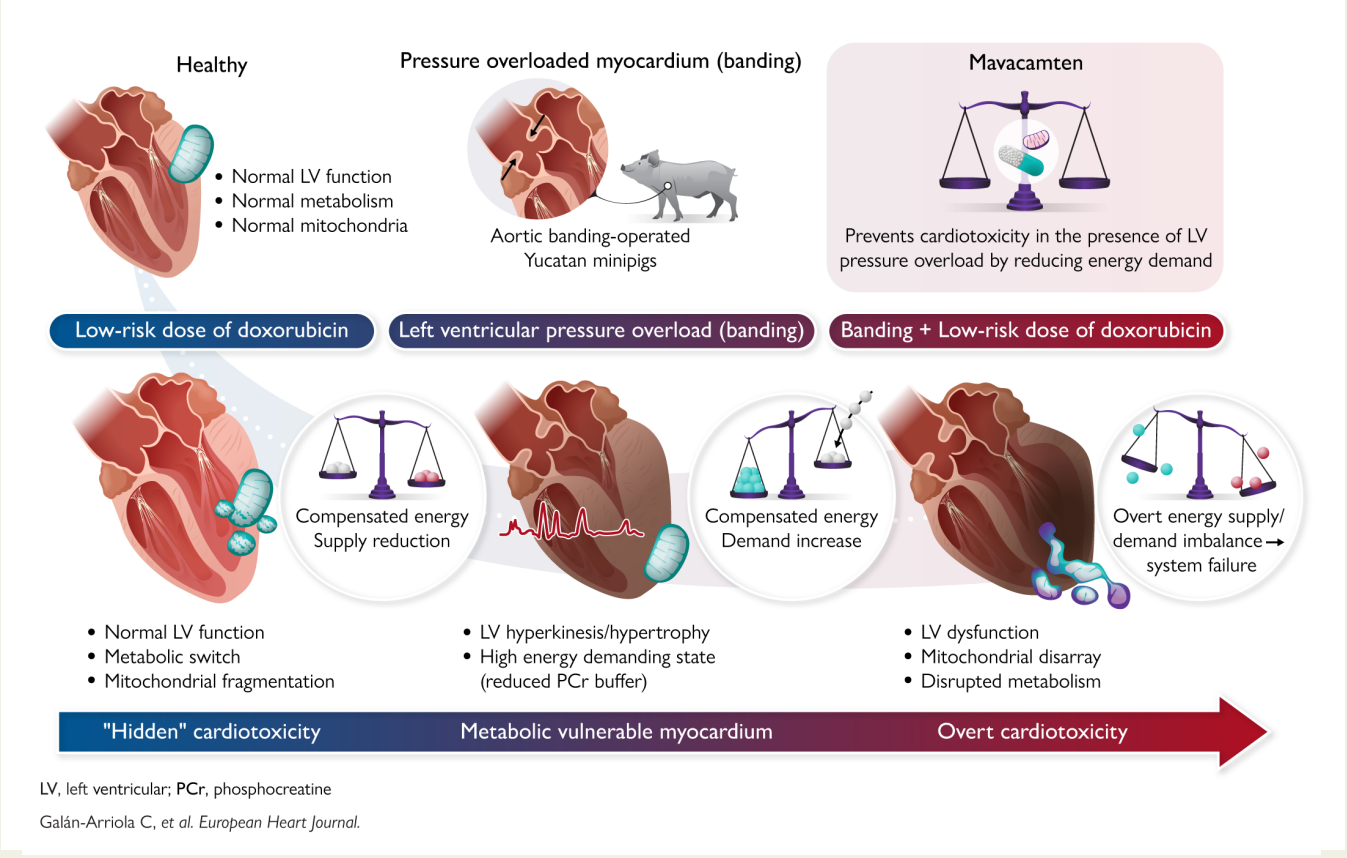

Experimental study showing that pre-existing left ventricular (LV) pressure overload induces a hypermetabolic myocardial state with preserved systolic function but reduced energetic reserve. In this setting, exposure to low-dose doxorubicin precipitates mitochondrial dysfunction, myocardial fibrosis, and overt LV dysfunction, leading to reduced survival. *In vitro*, pharmacological reduction of myocardial energy demand with mavacamten prevents anthracycline-associated cardiotoxicity, likely through restoration of energetic balance. The latter supports an energy mismatch-driven mechanism and identifying myocardial energetic modulation as a potential protective strategy in patients with pressure-overloaded hearts.

Keywords Cardiooncology • Anthracyclines • Heart failure • MR spectroscopy

Translational Perspective

Anthracycline cardiotoxicity remains a major concern in cancer survivors. Epidemiological evidence indicates that patients with pre-existing left ventricular (LV) pressure overload (e.g. hypertension) are at increased risk. Evidence from this study demonstrates that LV pressure overload induces a high-energy-demand state, creating a latent metabolic vulnerability that predisposes the heart to dysfunction upon anthracycline exposure. Therapeutic strategies aimed at reducing myocardial energy demand—such as pharmacological contractility modulation (myosin inhibitors)—were shown to mitigate this vulnerability. These insights support the recognition of LV pressure overload as a key risk factor and highlight myocardial energetic imbalance as a modifiable target for preventing anthracycline cardiotoxicity in patients with cardiovascular comorbidities.

Anthracycline cardiotoxicity, also termed anthracycline-induced cardiotoxicity (AIC), is a clinically significant problem that has a profound impact on cancer survivors who, after successful chemotherapy, experience severe secondary cardiovascular effects that limit their quality of life.[1,2] Current clinical guidelines emphasize the importance of identifying and managing risk factors predisposing to AIC.[3] A recently validated tool for AIC risk assessment is the HFA-ICOS score, which incorporates various cardiovascular disease factors, including hypertension, valvular disease, and ventricular dysfunction.[4,5] Although the association between these clinical variables and AIC risk has been well established in epidemiological studies, the underlying mechanisms through which these factors contribute to increased risk remain poorly understood. Elucidating these underlying mechanisms is essential for the development of effective preventive therapies.[6]

Two of the main clinical risk factors for AIC are hypertension—especially when accompanied by left ventricular (LV) hypertrophy[7–11]—and significant valvular heart disease.[12] Both these conditions are characterized by LV pressure overload, but despite the well-established association between elevated AIC risk and conditions featuring LV pressure overload, experimental research in this area has been limited to anecdotal studies in small animal models.[13] Given the high prevalence of LV pressure overload (mainly associated with hypertension), there is an urgent need for research in clinically relevant models to determine the mechanisms underlying this relationship and eventually to advance preventive strategies for AIC.

To address this knowledge gap, we investigated the impact of LV pressure overload on the development of cardiac dysfunction after exposure to low-risk anthracycline doses in a porcine large-animal model that is anatomically and physiologically similar to humans. We conducted a comprehensive longitudinal study combining multimodal imaging (including assessments of cardiac energetics) with advanced proteomic and mitochondrial function analyses to track cardiac structure, function, metabolism, and energetics over a long follow-up period. Complementary pharmacological studies *in vitro* were conducted to examine the mechanistic role of energetic imbalance.

Methods

Study design

All procedures conformed to the European Directive 2010/63/EU on the protection of animals used for scientific purposes and were approved by the institutional animal care and use committees under three successive protocols (PROEX 074/15, PROEX 001/19, and PROEX 23.8/25). The census data of the animals that completed the protocol are summarized in Supplementary data online, *Table S1*. The study design is summarized in *Figure 1*. At the beginning of the protocol, 2-month-old Yucatan minipigs (females and castrated males) were randomized to aortic banding to induce LV pressure overload or to no operation. Four months after surgery (M4), animals were further randomized to vehicle or a low-risk dose of doxorubicin (5 weekly 1 mg/kg i.v. injections), dose selected based on a previous dose–response study. This resulted in four experimental groups: (i) Control (Ctrl) group: no operation, no anthracycline exposure; (ii) Doxorubicin (Dox) group: no operation plus low-risk anthracycline regimen; (iii) Banding (B) group: LV pressure overload, no anthracycline exposure; and (iv) Banding + Doxorubicin (B + Dox) group: LV pressure overload plus low-risk anthracycline regimen. After completion of the doxorubicin/vehicle injections, all animals were followed up until 8 months after aortic banding/no operation (4 months after the first injection of doxorubicin/vehicle) and then sacrificed for tissue harvesting and *ex vivo* analysis. From the beginning of the study, all animals underwent serial *in vivo* multimodality imaging studies, including multiparametric cardiac magnetic resonance (CMR), MR spectroscopy, and ^{18}FDG positron emission tomography (PET). Invasive haemodynamic assessment by Swan-Ganz catheterization was performed before initiation of anthracyclines (at time M4) and at the end of the study (M8).

The mechanistic involvement of high-energy demand cardiac deterioration upon doxorubicin exposure was evaluated *in vitro* exposing HL1 cardiomyocytes to isoproterenol and doxorubicin with/out pre-treatment with the selective myosin inhibitor mavacamtem.

Generation of left ventricular pressure overload

Aortic banding was induced surgically by placing a band around the ascending aorta.[14,15] Further details can be found in supplementary material.

Systemic low-risk dose anthracycline administration

All animals in the Dox and B + Dox groups received 1 mg/kg intravenous doxorubicin. The dose was identified in a dose–response study performed in an independent set of animals (see Supplementary data online, *Figure S1A*). Additional information for doxorubicin injections can be found in supplementary material.

Animal care and humanitarian endpoint criteria can be found in supplementary material.

Definition of cardiotoxic events

In addition to the analysis of the impact of interventions on cardiac systolic function as a continuous variable, animals were classified as having experienced a cardiotoxic event on the basis of the LVEF criteria outlined in the recent ESC Cardio-Oncology guidelines.[3] Severe cardiotoxicity was defined as an LVEF below 40%, while moderate cardiotoxicity was defined as an LVEF below 49% or a decrease of 10% points from baseline.

Cardiac magnetic resonance and magnetic resonance spectroscopy

All CMR studies were conducted with a Philips 3-T Achieva Tx whole-body scanner (Philips Healthcare, Best, The Netherlands) equipped with a 32-element phased-array cardiac coil. Information about CMR acquisition protocol and analysis can be found in supplementary material.

Data obtained from cardiac-ECG-triggered localized ^{31}P-MRS data were obtained for the non-invasive assessment of human myocardial high-energy phosphate metabolism (see supplementary material for additional information).

Positron emission tomography/computed tomography

All studies were performed with a GEMINI TF 64-slice PET/CT scanner (Philips Healthcare, Best, the Netherlands). Additional information can be found in supplementary material.

Cardiac catheterization

Right and left heart catheterizations were performed at the two specified time points (months 4 and 8) to assess intracavitary and pulmonary pressures. Following sedation as described above, vascular access was obtained via the femoral artery and vein using an ultrasound-guided Seldinger technique. After establishing access, a Swan-Ganz catheter was inserted via the venous route to measure pressures in the right atrium, right ventricle, pulmonary artery, and pulmonary capillary wedge positions. For arterial access, a pigtail catheter was advanced across the banding into the left ventricle to obtain pressure measurements.

Statistical methods

Sample size calculation and expanded statistical section are detailed in supplementary material. Data are presented as mean ± standard deviation or median with interquartile ranges, depending on their distribution.

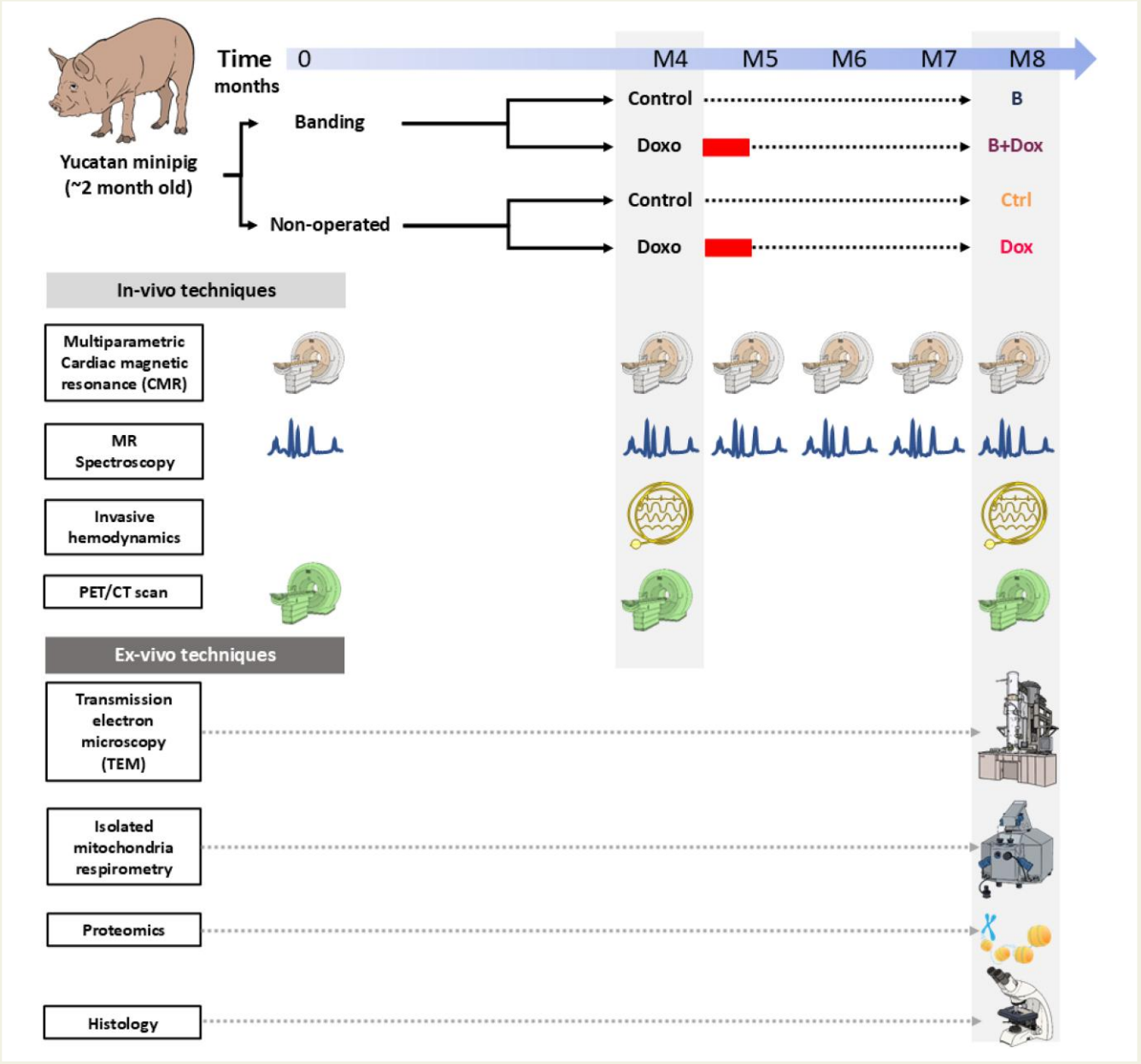

Figure 1 Study design. Study protocol, including sample size for each experimental group at the beginning and end of follow-up. Icons indicate *in vivo* techniques (cardiac magnetic resonance, positron emission tomography/computed tomography, magnetic resonance spectroscopy, Swan-Ganz catheterization, and blood sampling) and *ex vivo* techniques (transmission electron microscopy, OROBOROS, histology, and proteomics)

Normality was assessed using the Shapiro–Wilk test. For comparisons between multiple groups, a one-way a Wilcoxon (paired or unpaired) test was used. Kaplan–Meier survival curves were generated. Box plots depict the median, with whiskers representing the first and third quartiles. Statistical significance was defined as $P < .05$, with *P*-values adjusted for multiple comparisons where applicable. All statistical analyses and data visualizations were conducted using RStudio (version 4.3.0 (2023-04-21 ucrt); RStudio Team, Boston, MA, USA), an integrated development environment for R. The data were processed and analysed with various packages from the tidyverse collection (Wickham *et al*., 2019), including dplyr for data manipulation, ggplot2 for visualizations, and tidyr for data tidying.

Complete information for histology, transmission electron microscopy (TEM), high-resolution respirometry, glycogen content analysis, proteomics, and cardiomyocytes cell culture experiments can be found in supplementary material.

Results

Left ventricular pressure overload activates a subclinical cardiac energetic reprogramming to sustain myocardial function

At the beginning of the study protocol, LV pressure overload was induced surgically in 2-month-old pigs by placing a band around the

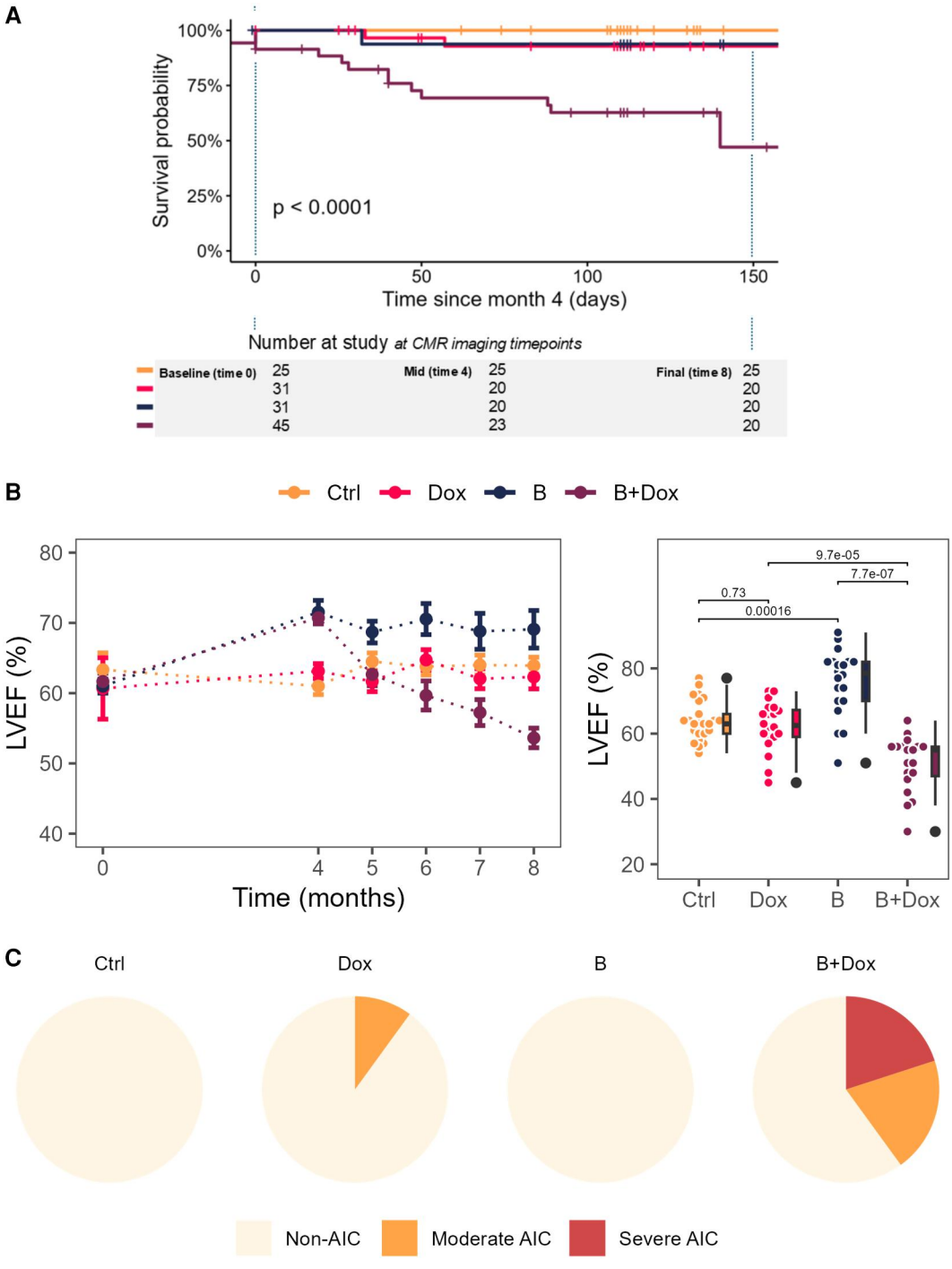

Figure 2 Cardiac function and anthracycline cardiotoxicity in the swine model. (*A*) Kaplan–Meier survival curve for each experimental group (dead secondary to humanitarian sacrifice due to bad condition or severe myelosuppression is considered as censored time). (*B*) *Left*, Left ventricular ejection fraction trajectories over the study period (mean and standard error). *Right*, Individual and grouped data per group 4 months after the initiation of doxorubicin/vehicle. Data points represent individual animals. Boxes show the interquartile range with the median line, and whiskers extend to the minimum and maximum values, excluding outliers. (*C*) Pie chart representing the percentage of animals showing signs of anthracycline cardiotoxicity (ESC cardio-oncology guideline criteria) at the end of the study. Ctrl, non-operated plus vehicle; Dox, non-operated + low-risk doxorubicin regimen; B, LV pressure overload induced by aortic banding; B + Dox, aortic banding followed by doxorubicin exposure

ascending aorta to produce supravalvular aortic stenosis (see Supplementary data online, *Figure S1A*). Among pigs receiving no subsequent anthracycline treatment, no casualties were recorded during the 8 months after aortic banding (B group) or no operation (Ctrl group) (*Figure 2A*). At 4 months after surgery, LV mass was significantly greater in pigs with aortic banding than in non-operated animals (79.7[33.7] g vs

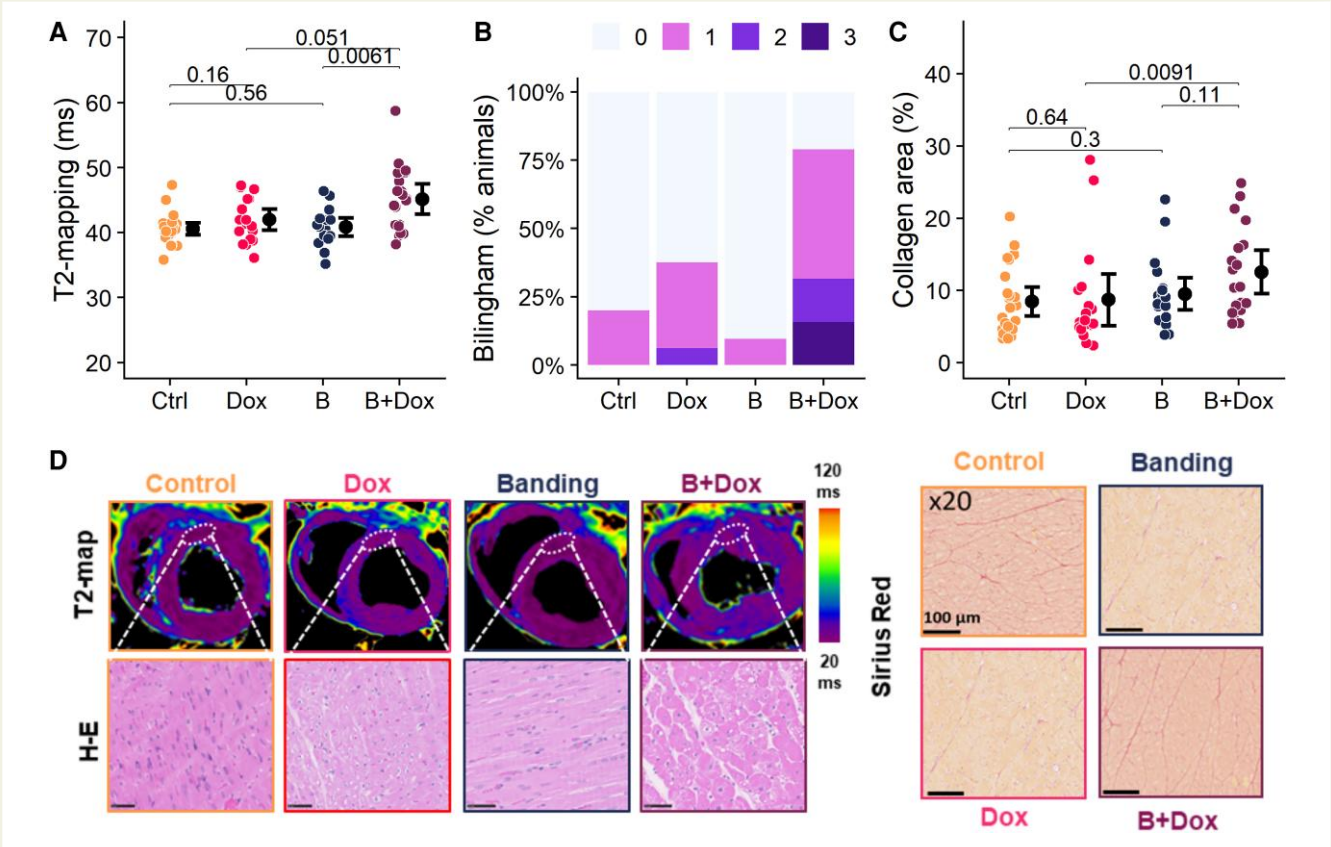

Figure 3 Myocardial tissue characterization. (*A*) End-of-study T2-GraSE mapping in the mid-anterior LV wall. (*B*) Billingham score stacked barplot indicating the proportion of animals with intra-cardiomyocyte vacuolization detected by HE staining. (*C*) Collagen fraction area indicating the extent of myocardial fibrosis, measured with an automated macro from Sirius Red staining in the mid-anterior LV slice. (*D*) Representative images from cardiac magnetic resonance T2 sequences (*left*, *top row*), HE staining (*left*, *bottom row*), and Sirius Red staining (*right*). Data points in *A* and *C* represent individual animals. Bars represent mean and standard deviation. Ctrl, non-operated plus vehicle; Dox, non-operated + low-risk doxorubicin regimen; B, LV pressure overload induced by aortic banding; B + Dox, aortic banding followed by doxorubicin exposure

45 [12.6] g, $P < .0001$), and this was accompanied by significant elevations in LVEF (73 [9.5] % in B group vs 59 [7] % in Ctrl, $P = .0081$) and stroke volume (58.7 [17.6] mL vs 38 [15.1], $P = .02$) (*Figure 2B*, and Supplementary data online, table *S2*). Cardiac catheterization confirmed the characteristic changes associated with LV pressure overload, with LVEDP significantly higher in banded pigs (8 mmHg [3.5] B vs 5 mmHg Ctrl [3], $P = .035$). Mean pulmonary capillary wedge pressure (PCWP) and right atrial pressure (RAP) were 8 mmHg [4.8] vs 6 mmHg [3.8] ($P = .2$) and 4 mmHg [1.8] vs 2 mmHg [7] ($P = .31$), respectively (see Supplementary data online, table *S3*). Trans-banding aortic gradient and aortic velocity significantly increased after surgery (see Supplementary data online, *Figure S2C–D*). On histology, left atrium from pigs with LV pressure overload had a significant increase in fibrosis (see Supplementary data online, *Figure S2A*). Cardiomyocyte area and proteomic markers of hypertrophic response were significantly increased (see Supplementary data online, *Figure S2E–G*). No changes were observed in LV fibrosis (*Figure 3C*). At time M4, banded and non-operated animals randomized to the non-anthracycline study arm (B and Ctrl groups, see *Figure 1*) received injections of vehicle and were followed up until the end of the study (M8). At the study endpoint, the LVEF elevation in banded pigs was maintained (78.5% [12.0] B vs 63.0% Ctrl [7.0], $P = .00019$. *Figure 2B*), as was the LVEDP elevation, and the elevations in pulmonary wedge and right atrial pressures were statistically significant. Complete CMR and haemodynamic data for both timepoints are shown in Supplementary data online, tables *S2* and *S3*. The LV pressure overload phenotype was not accompanied by significant increases in extracellular space, oedema, or fibrosis detected by CMR or histology (*Figure 3*). PET analysis of myocardial glucose uptake detected no difference between banded and non-operated pigs (*Figure 4A and B*). No accumulation of lipid or glycogen droplets was observed on TEM, and neither mitochondrial structure (TEM) nor function (respirometry) differed between the two conditions (*Figure 4C–G, I and J*).

In vivo assessment of cardiac energetics by magnetic resonance spectroscopy (MRS) revealed significantly altered cardiac energetics in pigs with LV pressure overload. Although ATP content remained stable in banded pigs, phosphocreatine (PCr) was significantly reduced vs non-operated controls (24.1 [12.0] B vs 32.65 [11.27] Ctrl, $P = .022$) (*Figure 4H*). These data suggest that the myocardium copes with the high-energy demand brought on pressure overload by preserving the immediate energy pool (ATP) at the expense of consuming the PCr reserve.

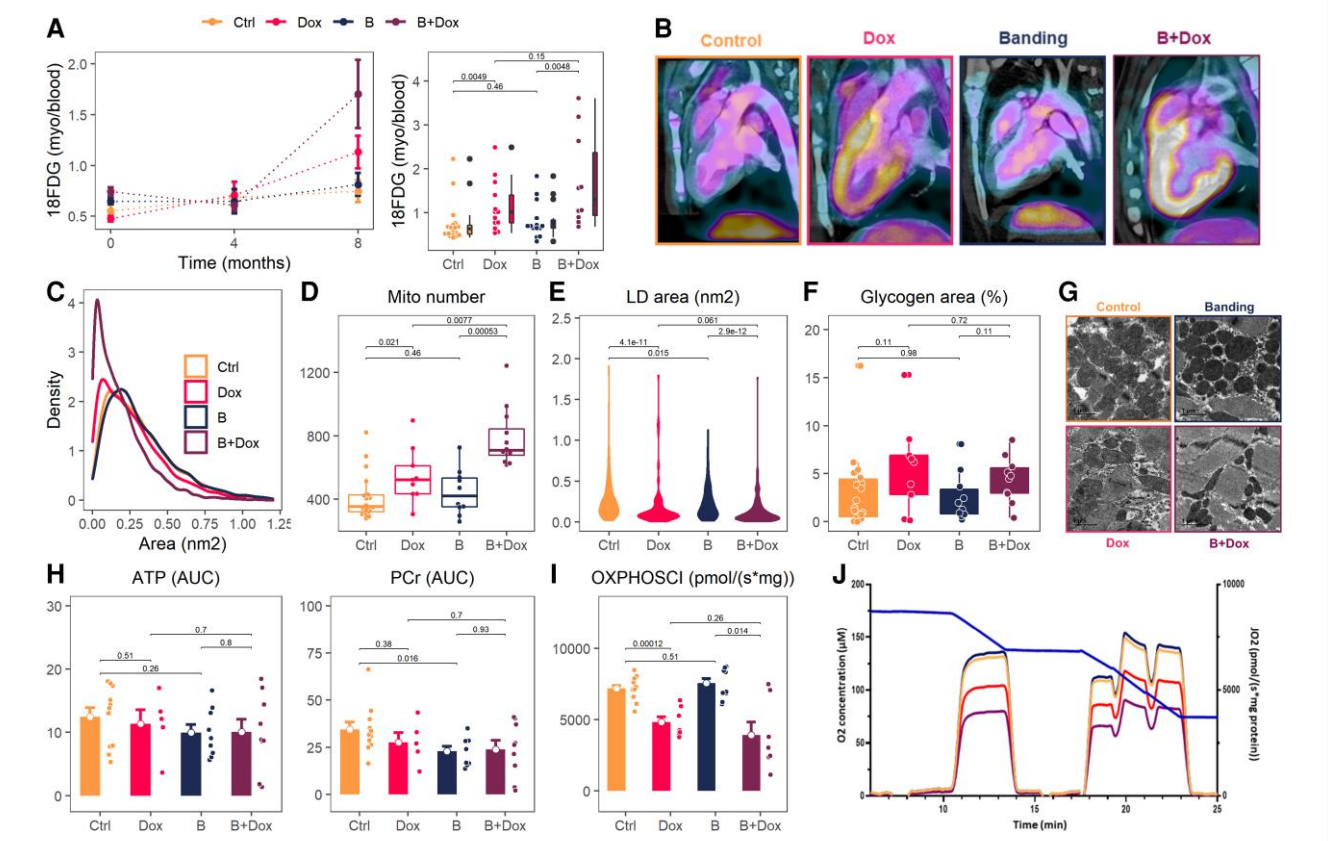

Figure 4 Cardiac metabolic function. (*A*) *Left*, Positron emission tomography/computed tomography analysis of myocardial glucose (^{18}FDG) uptake trajectories (mean and standard error). *Right*, Individual and grouped data per group at the end of the study; data points represent individual animals. Boxes show the interquartile range with the median line, and whiskers extend to the minimum and maximum values, excluding outliers. (*B*) Representative positron emission tomography/computed tomography contrast images at the end of the study. (*C*) Density plot of mitochondrial size distribution at the end of the study. (*D*) Mitochondrial number measured from transmission electron microscopy images at the end of the study. (*E*, *F*) Violin plots of the lipid droplet area (*E*) and glycogen content (*F*) by transmission electron microscopy. (*G*) Representative transmission electron microscopy images showing mitochondrial shape and size. (*H*) Magnetic resonance spectroscopy analysis of ATP and phosphocreatine content (areas under curve). (*I*) Myocardial mitochondrial respiratory function in freshly isolated mitochondria. (*J*) Representative high-resolution mitochondrial respirometry (OROBOROS) experiment. Data points in H and I represent individual animals. Barplots represent means and standard error. Ctrl, non-operated plus vehicle; Dox, non-operated + low-risk doxorubicin regimen; B, LV pressure overload induced by aortic banding; B + Dox, aortic banding followed by doxorubicin exposure

Proteomic analysis showed that LV pressure overload induced myocardial up-regulation of protein clusters associated with high-energy demand, including proteins of the tricarboxylic acid (TCA) cycle, calcium signalling, and actin cytoskeleton regulation (*Figure 5A*). These adaptations suggest that the response to LV pressure overload involves enhanced metabolic activity and structural reorganization. LV pressure overload did not trigger any notable disruption in mitochondrial respiratory complex CI and glycolysis, indicating that mitochondrial function and energy production capacity were preserved under these conditions.

These data suggest that moderate LV pressure overload generates a metabolically stressed myocardium as an adaptation to preserve cardiac performance and withstand the increased afterload. Metabolic homeostasis and mitochondrial function are maintained, ensuring immediate ATP availability, but at the cost of a reduced energy reserve. Under these conditions, the heart continues to function without manifesting signs of failure.

Absent high-energy demand, cardiac metabolic changes induced by a 'low-risk' cumulative anthracycline dose do not impair cardiac function

To study the interaction between pressure overload and anthracycline exposure, we sought a doxorubicin regimen that on its own does not cause overt cardiac dysfunction. Doxorubicin (5 weekly 1 mg/kg i.v.) or vehicle injections were initiated at M4 in non-operated pigs that were then followed up for 4 months from the time of the first injection (*Figure 1*).

Among pigs receiving doxorubicin injections for 4 months without LV pressure overload, mortality at the end of the study was 7% (*Figure 2A*). LV mass, LV volume, and LVEF did not differ between the doxorubicin-only (Dox) and vehicle-only (Ctrl) groups at any point during follow-up (*Figure 2B* and Supplementary data online, table *S2*). Only 19% of Dox-treated pigs met the LVEF-based ESC 2022 cardio-oncology

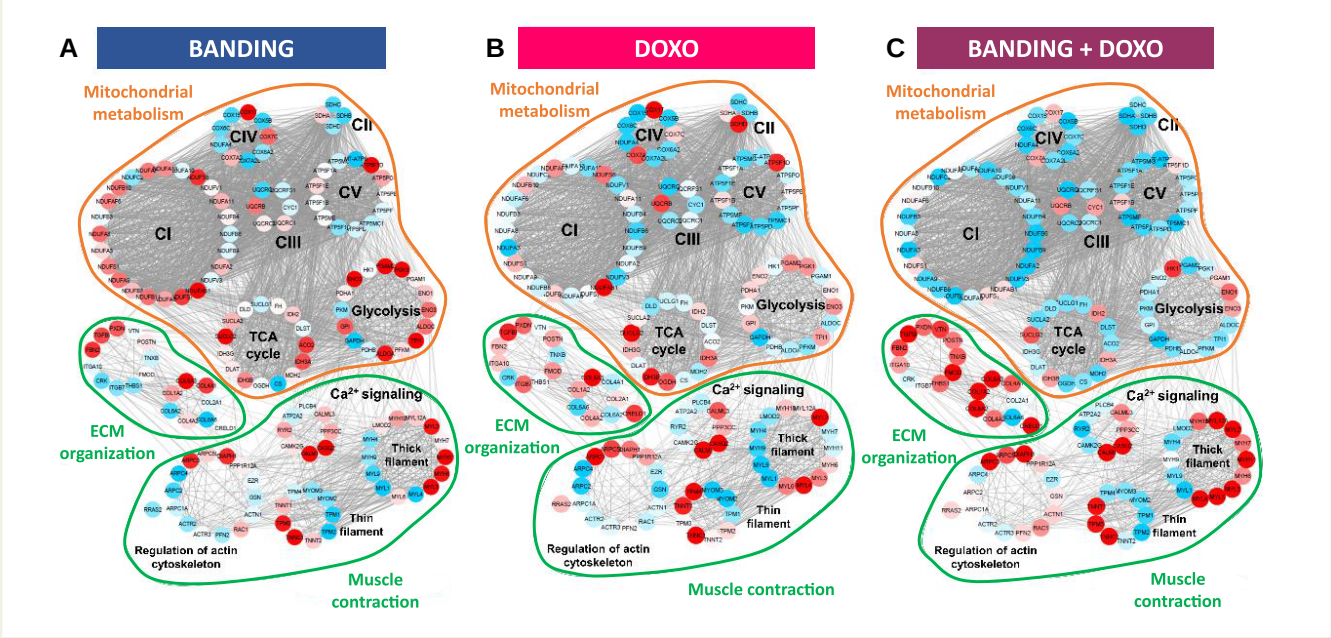

Figure 5 Proteomic footprint. High-throughput multiplexed quantitative proteomics was performed in myocardial tissue of 16 randomly selected animals (4 per experimental group) to detect protein abundance changes in (*A*) banding, (*B*) doxorubicin and (*C*) banding + doxorubicin groups in comparison to the control group. Protein quantitative data were then analysed using the Systems Biology Triangle model[16] (ref) to detect coordinated protein abundance changes within functional categories. Protein–protein interaction networks were built for functional categories found significantly altered (FDR < 0.05) in at least one group. Each node represents a protein, and the edges (lines) between nodes indicate interactions or associations between the proteins. The colour code indicates the protein abundance change (up-regulated in red and down-regulated in blue), reported as the standardized log2 fold-change (Zq) with respect to the control group. Functional protein clusters are highlighted: mitochondrial metabolism (mitochondrial respiratory complexes CI, CII, CIII, CIV, and CV; tricarboxylic acid cycle; glycolysis); extracellular matrix organization, and muscle contraction (Ca^{2+} signalling; regulation of actin cytoskeleton; sarcomere thin and thick filaments). Protein–protein associations were taken from the STRING database (ref).[17] The complete set of proteins and functional categories quantified in this comparative analysis is provided in Supplementary data online, *Table S4*

guideline criteria for moderate cardiotoxicity (*Figure 2C*). Similarly, Dox-group pigs showed no differences from the Ctrl group for any CMR parameter, including T1 and T2 mapping (*Figure 3A*, Supplementary data online, table *S2*). The absence of any functional impact of low-risk doxorubicin treatment was confirmed by cardiac catheterization, with all parameters showing no differences between the Dox and Ctrl groups at end of follow-up (see Supplementary data online, table *S3*).

Histological examination revealed mild cardiomyocyte vacuolization, a characteristic feature of early anthracycline cardiotoxicity,[18] in Dox-group pigs (*Figure 3B and D*).[18] Consistent with the T1 mapping data, Sirius Red staining showed no between-group differences in fibrosis (see Supplementary data online, *Table S2*, and *Figure 3C*), indicating that the early myocardial injury was primarily cellular (restricted to cardiomyocytes) and did not involve extensive extracellular matrix remodelling.

The low-risk anthracycline dose was associated with significant changes in myocardial substrate utilization. PET-CT analysis of ^{18}F-FDG uptake revealed significantly increased cardiac glucose uptake in doxorubicin-treated pigs compared with controls (0.886 [0.51] Dox vs 0.627 [0.20] Ctrl, $P = .014$) (*Figure 4A and B*). The increased glucose uptake was accompanied by a parallel reduction in myocardial lipids detected by TEM, which revealed a reduction in lipid droplet (LD) area to 0.094 nm^2 [0.122] in the Dox group, compared with 0.19 nm^2 [0.194] in the vehicle-treated Ctrl group ($P < .0001$) (*Figure 4E*). TEM also revealed fragmentation of cardiomyocyte mitochondria in doxorubicin-treated pigs since mitochondrial number per cell were increased in Dox (521 [176] vs 406 [121] in Ctrl, $P = .039$). Mean mitochondrial size were 0.224 nm^2 [0.289] and 0.291 nm^2 [0.311] in Dox and Ctrl respectively ($P = .1$) (*Figure 4C, D, and G*). These ultrastructural changes were accompanied by a reduction in mitochondrial respiratory capacity to 4266.6 pmol/(*smg*) [1533], compared with 7226 pmol/(smg) [978] in controls ($P = .0046$) (*Figure 4I and J*). Despite these subtle changes in metabolic substrate utilization and mitochondrial structure and function, *in vivo* MRS revealed no alteration in cardiac energetics (*Figure 4H*).

The proteomic analysis confirmed the metabolic shift from oxidative phosphorylation to anaerobic glycolysis in doxorubicin-exposed pigs, with proteins involved in oxidative phosphorylation (CI to CV) down-regulated, and glycolytic enzymes up-regulated (*Figure 5B*). Lipid oxidation was diminished compared with the rest of the conditions. Changes in calcium signalling pathways were also observed, suggesting early disruption of cellular homeostasis.

These data show that the low-risk doxorubicin dose induced early subclinical signs of mild AIC, evidenced by subtle changes in cardiac metabolism and mitochondrial function. Despite these early metabolic alterations, there was no detectable impact on cardiac anatomy or haemodynamic function. This suggests that the modified energy production system in doxorubicin-exposed hearts was sufficient to maintain cardiac function with no deterioration in cardiac energetics in the absence of additional cardiac stressors.

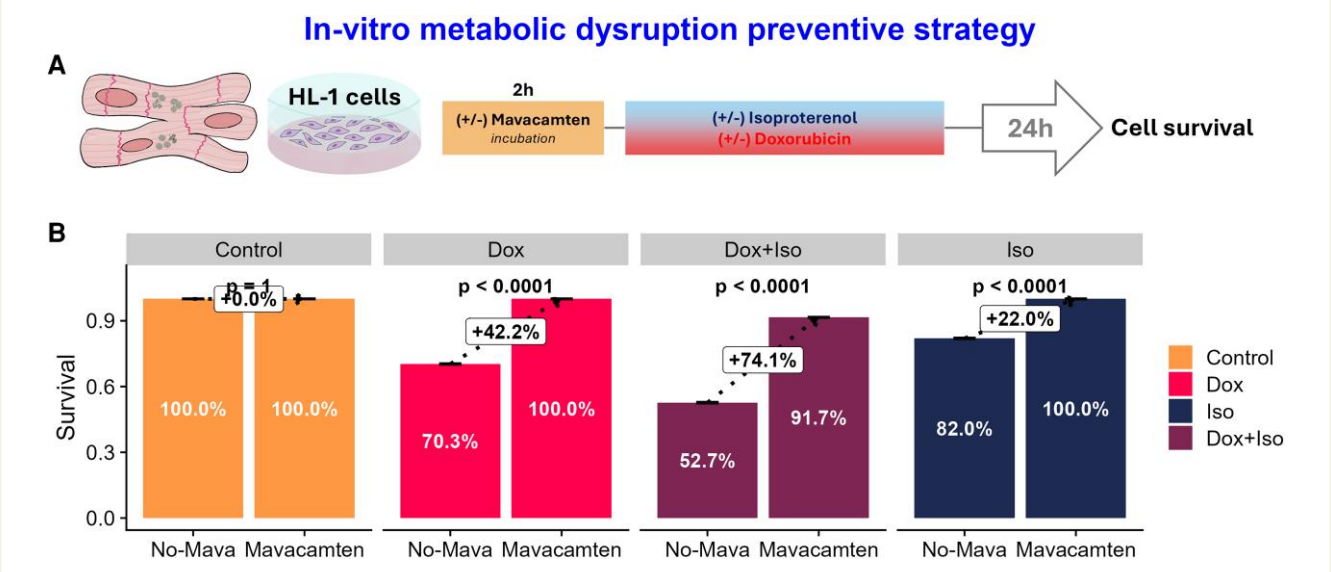

Figure 6 *In vitro* pharmacological metabolic modulation. (*A*) Experimental design: HL-1 cardiomyocytes were pre-treated (±mavacamten, 2 h), then incubated (±doxorubicin, ±isoproterenol) for 24 h; cell survival was quantified. (*B*) Survival bar plots by condition and treatment. Data shown as paired values per animal or replicate; Point and error bars represent mean and standard error. Coloured lines connect matched data. Bars reflect survival percentages; *P*-values shown per group

A low-risk cumulative anthracycline dose significantly disrupts cardiac homeostasis in pigs with pre-existing left ventricular pressure overload

The effect of a pre-existing high metabolically stressed myocardium on the response to low-risk cumulative anthracycline dosing was tested in pigs randomized to the doxorubicin protocol 4 months after surgical induction of LV pressure overload (*Figure 1*). Contrasting the high survival rates of pigs exposed to only one of these stressors, mortality in banded pigs further exposed to doxorubicin (B + Dox) was significantly increased at the end of the study ($P < .0001$ for the comparison with pigs exposed to either of the two stressors independently) (*Figure 2A*).

Pigs receiving low-risk cumulative doxorubicin dose after LV pressure overload induction showed a rapid and significant decrease in LVEF at the end of the 1-month doxorubicin protocol, from 72% [7.2] immediately before the doxorubicin regimen to 62% [13.5] immediately after ($P = .0002$). LVEF continued to decline thereafter, reaching its lowest recorded point (53% [11]) at the end of the study ($P < .0001$ vs immediately before doxorubicin initiation) (*Figure 2B*, left). At the end of the protocol, LVEF was significantly lower in the B + Dox group than in the B group, with LV pressure overload alone ($P < .0001$), or the Dox group, exposed to doxorubicin alone ($P = .00017$) (*Figure 2B*, right). Within the B + Dox group, 35% of pigs met the LVEF-based ESC 2022 cardio-oncology guideline criteria for cardiotoxicity, categorized as severe in half of these pigs (*Figure 2C*). Haemodynamic measurements in the B + Dox group revealed significant deterioration compared with the Dox only group (see Supplementary data online, Table *S3*).

In vivo tissue characterization by T2 mapping detected no alterations in pigs exposed to LV pressure overload or doxorubicin alone, whereas the B + Dox group showed significant T2 relaxation time prolongation, indicating oedema ($P = .0061$ and $P = .063$ vs the B and Dox groups, respectively) (*Figure 3A and D*). The *in vivo* T2 mapping data were consistent with the results of *ex vivo* histology, which revealed a significant increase in the density of myocardial vacuoles and a worse Billingham score in the B + Dox group (*Figure 3B and D*). Pigs in the B + Dox group also showed a significant increase in extracellular space measured by T1-mapping, consistent with the presence of fibrosis detected by *ex vivo* Sirius Red staining (see Supplementary data online, *Table S2* and *Figure 3C*). These data suggest that the combination of LV pressure overload and anthracycline administration not only affected cardiomyocytes but also involved significant extracellular matrix remodelling, contributing to the impaired cardiac function.

PET-measured ^{18}FDG uptake was further increased (albeit not reaching statistical significance) in the B + Dox group compared with pigs receiving doxorubicin alone (*Figure 4A and B*), indicating that the presence of LV pressure overload exacerbated the altered substrate utilization triggered by the doxorubicin regimen. This intensified shift in substrate utilization was paralleled by a more pronounced reduction in myocardial LD density on TEM (*Figure 4E*). Mitochondrial fragmentation was especially pronounced, with median mitochondrial size reduced to 0.141 nm^2 [0.212] compared with 0.224 nm^2 [0.289] in pigs receiving doxorubicin only ($P = .0093$) and mean mitochondrial number increasing to 708 [166] (vs 521 [176], $P = .0077$) (*Figure 4C, D, and G*). The combination of anthracycline stress with background LV pressure overload also severely reduced mitochondrial respiratory capacity, to 3024 pmol/(smg) [3016] in the B + Dox group vs 7633 pmol/(*smg*) [1578] in the banded group ($P < .05$) (*Figure 4I and J*). MRS analysis of cardiac energetics revealed that pigs in the B + Dox group had a significantly reduced myocardial PCr buffer, limiting the capacity to buffer fluctuations in ATP demand (*Figure 4H*).

The proteomics interaction-network assessment demonstrated disruptions in multiple pathways in B + Dox animals compared with pigs exposed to only one of the stressors (*Figure 5C*). There was significant down-regulation across all mitochondrial respiratory complexes (CI to

CV) and glycolytic enzymes, indicating an incapacity to use even glucose that results in storage of glycogen in the cardiomyocyte (*Figure 4F*) due to severe mitochondrial dysfunction. The B + Dox group also showed alterations in calcium signalling, extracellular matrix and cytoskeletal regulation pathways, indicating overtly disrupted cellular homeostasis, impaired contractile function, and fibrotic remodelling, which were not observed in the single-stressor groups.

Modulation of energetic stress to reveal imbalance between cardiac energy demand and production

To further support our hypothesis that the dual hit arises from a mismatch between increased energetic demand and impaired ATP production, we performed *in vitro* experiments.

To test whether reducing energetic demand could mitigate injury, we used HL-1 cardiomyocytes exposed to acute stressors (*Figure 6A*). Isoproterenol or doxorubicin alone modestly reduced cell survival (82% and 70.3%, respectively), while their combination markedly decreased viability (52.7%). Notably, mavacamten pre-treatment significantly improved survival across all groups; in the most severe condition (doxorubicin + isoproterenol), viability increased to 91.7% ($P < .05$ vs untreated), supporting the protective effect of demand reduction under stress mimicking LV pressure overload and chemotherapy exposure (*Figure 6B*).

Discussion

The results presented here show that whereas neither LV pressure overload nor low-risk anthracycline treatment alone affected cardiac function, the administration of a low-risk anthracycline dose against a background of pre-existing LV pressure overload led to rapidly progressing cardiac dysfunction. LV pressure overload alone induced a myocardial state of high-energy demand, which remained balanced in the absence of anthracyclines. However, this balance was undermined by anthracycline-mediated disruption of cardiac metabolism and mitochondrial function, leading to system failure and the onset of heart failure.

The main findings of our study are as follows:

(1) Aortic banding (supravalvular aortic stenosis) induced a marked increase in LV mass and stroke volume, accompanied by hyperkinetic LV global motion. The myocardium responded to the LV pressure overload by activating compensatory mechanisms that maintained overall cardiac function despite the increased energy demands. The PCr pool was depleted to maintain stable myocardial ATP content, reflecting well-preserved energy reserves and overexpression of proteins of the metabolic machinery. There was no significant fibrosis or extracellular matrix remodelling, and mitochondrial structure and function were maintained, suggesting that the myocardium adapted its metabolism without any overt dysfunction. These mechanisms resulted in a 'hidden' metabolic vulnerability in the heart.

(2) Exposure to the low-risk doxorubicin dose alone produced no notable changes in cardiac function or contractility. While a small percentage of animals showed subclinical signs of AIC, there were no significant LVEF alterations or extracellular matrix remodelling. Metabolic analysis revealed a switch in the preferential substrate from fatty acids to glucose. Increased glucose uptake and depletion of myocardial lipid stores were associated with early signs of mitochondrial structural and functional damage (fragmented mitochondria and reduced respiratory capacity), despite overall preserved cardiac energetics. The proteomics analysis supported these findings, indicating a metabolic shift from oxidative phosphorylation to glycolysis.

(3) Administration of a low-risk anthracycline dose to animals with pre-existing LV pressure overload overwhelmed the compensatory mechanisms that maintained myocardial function in the presence of pressure overload alone, rapidly leading to a significant decline in cardiac function and a marked increase in mortality. Histological analysis revealed extensive cardiomyocyte vacuolization, fibrosis, and oedema. Metabolic alterations were more pronounced, with further increases in glucose uptake and mitochondrial fragmentation, and a marked reduction in respiratory capacity. The proteomic analysis detected disruptions in mitochondrial respiratory complexes, metabolism and extracellular matrix remodelling.

(4) Pharmacological modulation of cardiac energetics confirmed that a mismatch between energy demand and production drives dysfunction. In *in-vitro* experiments, mavacamten pre-treatment—by reducing energy demand—significantly improved HL1 cardiomyocyte cell survival under combined mitochondrial and hypercontractile stress, highlighting the therapeutic potential of targeting energetic imbalance to prevent cardiac failure associated with anthracycline-induced mitochondrial damage. (*Structured Graphical Abstract*).

Although the clinical association between hypertension and cardiotoxicity is well recognized, experimental studies exploring the mechanistic basis remain limited, largely confined to small-animal models with short follow-up periods.[13,19,20] These studies, often using rodent models, have shown that pressure overload exacerbates anthracycline-induced cardiac dysfunction. However, the scope of these studies is limited due to the rapid development of cardiac dysfunction in rodents subjected to sustained pressure overload, making it challenging to assess the interaction between pressure overload and additional stressors like anthracyclines without the confounding effects of pre-existing systolic dysfunction. Furthermore, these studies did not consider the impact of either stressor (LV pressure overload and anthracycline administration) on cardiac metabolism and energetics and thus did not identify potential therapeutic targets for the prevention of this condition. Our study advances the field by utilizing a large-animal model that closely mimics human cardiovascular physiology. Unlike previous studies, we conducted a longitudinal assessment over a very long-term examination period (8 months) using a comprehensive set of clinical multimodal imaging techniques to track cardiac structure, function, metabolism, and energetics over time. We also performed detailed analyses of mitochondrial function and proteome changes, providing insight into the pathways disrupted by anthracycline exposure in animals with pre-existing LV pressure overload. These comprehensive evaluations demonstrated that while animals with LV pressure overload alone preserve cardiac function through metabolic compensation, even low-risk doses of anthracyclines destabilize this balance, rapidly leading to severe cardiotoxicity.

In the well-established pig model used here, aortic banding revealed a distinctive effect of pressure overload on the myocardium. This model has been widely used in the past to study cardiac adaptations to pressure overload, particularly through advanced imaging techniques.[14,15] It is important to highlight that the aortic banding generated in our model is mild-moderate (30% reduction in aortic perimeter). Thus, this model is closer to the LV pressure overload induced by systemic hypertension

in humans than by severe valvular disease. In fact, despite the impact on LV filling pressures and on cardiac energetics, the structural damage is very mild, with only increased fibrosis in the left atrium.[21] However, to our knowledge, it has not been used before to investigate the impact of LV pressure overload as a comorbidity on the response to anthracycline therapy. One of the key advantages of this model is that, despite inducing a significant and sustained pressure overload, as confirmed by haemodynamic measurements, it does not cause overt cardiac dysfunction. This feature enhances the translational relevance of the model, as it mirrors the clinical presentation of many hypertensive patients who exhibit pressure overload without manifesting significant systolic dysfunction.[22,23] The model thus allows exploration of interactions between pressure overload and additional stressors such as anthracyclines without confounding from pre-existing systolic dysfunction. This stands in contrast to smaller animal models, particularly rodents, in which prolonged pressure overload tends to result in cardiac dysfunction.[24,25] For example, the few available rodent studies investigating pressure overload in the context of cardiotoxicity showed that sustained pressure overload in rats eventually leads to cardiac dysfunction,[13,19,20] complicating the evaluation of combined insults. In our large-animal model, the absence of baseline cardiac dysfunction allowed us to isolate the effects of pressure overload on anthracycline-induced injury in a more clinically relevant setting.

The proteomic and MRS analyses provide clear evidence of a metabolically stressed myocardium under pressure overload, despite the preserved cardiac function. The up-regulation of the TCA cycle and calcium signalling pathways is consistent with a hypercontractile phenotype and aligns with previous studies of pressure overload that reported metabolic adaptations related to increased energy demand.[26–28] The spectroscopy findings, including a reduced PCr pool without a corresponding decrease in ATP content, further support the idea that increased afterload triggers a reprogramming of myocardial energetics, consistent with human studies.[29–36] Our results are in line with previous evidence that high-energy-demand situations produce a drop in PCr concentration to maintain myocardial ATP content.[29,37] This finding highlights the metabolic vulnerability of the pressure-overloaded myocardium due to its increased reliance on fatty-acid oxidation, since any further stress on this pathway, such as anthracycline exposure, can overwhelm this compensatory mechanism, leading to metabolic failure and subsequent cardiac dysfunction.

Our study design allowed us to examine the effects of a low-risk doxorubicin regimen in isolation. As our goal was to explore subclinical cardiotoxicity in a controlled manner, we selected a low cumulative doxorubicin dose that would not cause overt cardiac dysfunction when administered alone. Previous studies, including our own work in porcine and murine models, have shown that exposure to a low cumulative anthracycline dose causes metabolic reprogramming but without immediate impact on cardiac function,[18,36,38] with overt systolic dysfunction and cardiomyocyte damage occurring only when a higher cumulative anthracycline dose is reached. Several studies have highlighted the subclinical nature of many forms of AIC,[34] leading to the suggestion that early metabolic and mitochondrial alterations can accumulate over time, increasing the risk of heart failure later in life or upon exposure to additional stressors, an increasingly recognized phenomenon known as hidden cardiotoxicity.[39] Our study provides strong evidence for this idea, since the low cumulative anthracycline dose used induced metabolic changes that on their own generated no LV functional deterioration but in the presence of pre-existing LV pressure overload resulted in overt heart failure. The metabolic changes we observed, particularly the shift from oxidative phosphorylation to glycolysis and mitochondrial fragmentation, appear to be early signs of cardiotoxicity that predispose the myocardium to future dysfunction. These results also underscore the importance of detecting and monitoring these subtle metabolic changes, as they may provide early warning of AIC, even in patients who do not initially present with functional impairment. Furthermore, by using a low-dose regimen in a large-animal model, we were able to more closely replicate the clinical scenario, where patients receive anthracyclines at doses that are not immediately cardiotoxic but may affect heart health over the long-term. These early metabolic shifts may thus serve as biomarkers for AIC.

The combination of pressure overload with later anthracycline exposure overwhelmed the compensatory mechanisms observed for pressure overload alone, leading to a rapid deterioration in cardiac function. This suggests that the pressure-overloaded myocardium is already functioning at high-energy demand and has limited capacity to adapt supply. The addition of anthracycline therapy in this high-demand, low-supply situation compromises the energy supply by disrupting mitochondrial function, resulting in a mismatch between energy demand and ATP production and ultimately leading to heart failure. Only ~50% of pigs in the B + Dox group survived the study; therefore, metabolic, histological, and proteomic analyses reflect survivors and may underestimate mitochondrial dysfunction or fibrosis in the most severely affected animals. Moreover, as the pigs were enrolled prepubertally and reached adulthood during follow-up, baseline immaturity may have increased their susceptibility to combined stressors.

The reduced LVEF and other signs of heart failure in pigs exposed to both stressors (B + Dox) are insufficient to explain the striking increase in mortality in this animal group compared with the unaltered mortality rate in response to LV pressure overload or low-dose doxorubicin alone. It is therefore likely that the combined exposure to both stressors triggers additional cardiac dysfunction, beyond heart failure. We speculate that the combination of pressure overload and anthracycline therapy might increase the risk of malignant ventricular arrhythmia. An elevated risk of AIC has been reported in patients with genetic mutations associated with cardiomyopathies[40]; however, the arrhythmic risk in this at-risk patient group has so far not been investigated.

To mechanistically validate the hypothesis that anthracycline cardiotoxicity in pressure-overloaded hearts results from an energy supply–demand mismatch, we performed *in vitro* experiments in HL1 cardiomyocytes. Under isoproterenol stimulation, energy demand rose, but mitochondria damaged by anthracyclines could not increase ATP production, leading to cell death. In contrast, when cells were treated with mavacamten, a selective myosin inhibitor, the isoproterenol-induced rise in energy demand was blunted, maintaining a balance between supply and demand at lower levels. These findings, besides providing a mechanistic validation, identify myosin modulators as a potential therapeutic strategy for this condition.

Our findings open new therapeutic avenues for preventing AIC in patients with pre-existing LV pressure overload, such as those with hypertension or valvular heart disease. This situation places these patients at high risk and therefore in the greatest need of cardioprotective interventions.[2,41] One possible strategy suggested by our results for this patient group is PCr supplementation. A meta-analysis of several small randomized clinical trials suggested that i.v. PCr treatment can reduce hard outcomes in patients with various cardiac conditions[42]; however, this has not been tested in the context of anthracycline cardiotoxicity. Another possible intervention is chronic exercise training, since this has been shown to improve cardiac energy metabolism, enhancing mitochondrial efficiency and helping maintain stable PCr content even

during periods of intense demand.[43] This metabolic adaptation might be particularly beneficial in improving the resilience of the heart against stresses, including anthracycline exposure. Supporting this idea, a recent small clinical trial showed that 1-year exercise training produced large benefits in cardiorespiratory fitness and cardiac reserve in patients receiving anthracycline therapy.[44] Patients may also benefit from drugs that reduce myocardial energy demand, such as mavacamten, a selective cardiac myosin inhibitor that modulates contractility and reduces the energetic burden on the heart.[45,46] Another avenue for protection could be treatments that prevent the metabolic shift induced by anthracyclines. Strategies aimed at maintaining oxidative phosphorylation and preventing the shift towards glycolysis, or drugs that stabilize mitochondrial function, could mitigate the subclinical metabolic changes we observed in our study. This approach could prevent early mitochondrial damage and preserve energy production, thereby protecting the myocardium from the detrimental effects of anthracycline exposure in the presence of comorbidities. By addressing both the supply and demand sides of the myocardial energy balance, therapies such as these have the potential to improve outcomes for patients at high AIC risk.

Limitations of the study

The animal model used, despite being highly translational, does not recapitulate late-onset cardiotoxicity. Further studies first exposing animals to doxorubicin and later in time inducing comorbidities are needed. There is a lack of standard cardiotoxic cumulative doses of doxorubicin for large animal models. To compensate for this, we performed a pilot study to determine the dose to be used in the actual experiments. Second, while ours is the experimental study with the longest follow-up period reported to date, we did not address the clinically relevant very long-term impact of anthracycline exposure in combination with LV pressure overload on cardiac function and survival. Third, the findings, while relevant to humans, likely do not fully replicate the diversity of patient responses related to genetic, environmental, and lifestyle factors that could influence outcomes. Fourth, our study design did not allow us to investigate the potential mechanism responsible for the increased mortality in pigs exposed to both stressors. This important question should be investigated through electrophysiological studies. Fifth, while our model mimics chronic pressure overload, it does not account for other common cardiovascular comorbidities, such as diabetes or chronic kidney disease, which could further modulate the cardiotoxic response. Finally, since the model was associated with mortality across the study, final endpoint imaging and myocardial results might be affected by survival bias. However, this possible bias does not invalidate results since animals dying are expected to have shown more extreme differences compared to other groups.

Acknowledgements

We are deeply grateful to María Isabel Higuero-Verdejo for her exceptional work as a large-animal technician, and to the other animal-facility staff, especially Santiago Rodríguez Colilla, Inés Sanz Bueno, Tamara Córdoba, Antonio Benítez Sousa, Isabel Rodríguez Gómez, and Nicolás Cruz Zambrano, whose care of the animals was crucial to the success of this study. We also thank Braulio Pérez and Marta Gavilán for their support as imaging technicians, as well as the transmission electron microscopy unit at the Universidad Autónoma de Madrid and the microscopy unit at the CNIC, especially Verónica Labrador for her invaluable contribution. Lucía Pilar López Palomar for her technical work in the *in-vitro* experiments. Simon Bartlett (CNIC) provided English editing.

Supplementary data

Supplementary data are not available at *European Heart Journal* online.

Declarations

Disclosure of interest

Javier Sánchez-González is a Philips employee. All other authors declare no conflicts of interest.

Data Availability

The proteomics data are available at the PRIDE repository[47] (PXD056684). Additional data and code are available upon reasonable request.

Funding

European Commission (grant number ERC-CoG 819775 to B.I.), Spanish Ministry of Science and Innovation (PID2022-140176OB-I00 to B.I., PID2021-122348NB-I00 to J.V., PLEC2022-009235 to B.I., PLEC2022-009298 to D.S.), La Caixa (LCF/PR/HR22/52420019 to J.V.), and the Red Madrileña de Nanomedicina en Imagen Molecular -Comunidad de Madrid (P2022/BMD-7403 RENIM-CM). D.M.-H. is the recipient of a Doctoral INPhINIT Fellowship from la Caixa Foundation. The CNIC is supported by the Instituto de Salud Carlos III (ISCIII), the Ministerio de Ciencia, Innovación y Universidades, and the Pro CNIC Foundation and is a Severo Ochoa Center of Excellence (grant CEX2020-001041-S funded by MICIN/AEI/10.13039/501100011033).

Ethical Approval

All animal procedures were approved by the CNIC Institutional Animal Care and Use Committee and complied with national and European regulations.

Pre-registered Clinical Trial Number

Not applicable.

References

1. Moslehi JJ. Cardio-oncology: a new clinical frontier and novel platform for cardiovascular investigation. *Circulation* 2024;**150**:513–5. https://doi.org/10.1161/CIRCULATIONAHA.124.065473
2. Moreno-Arciniegas A, Cadiz L, Galan-Arriola C, Clemente-Moragon A, Ibanez B. Cardioprotection strategies for anthracycline cardiotoxicity. *Basic Res Cardiol* 2024;**120**:71–90. https://doi.org/10.1007/s00395-024-01078-6
3. Lyon AR, López-Fernández T, Couch LS, Asteggiano R, Aznar MC, Bergler-Klein J, *et al.* 2022 ESC Guidelines on cardio-oncology developed in collaboration with the European Hematology Association (EHA), the European Society for Therapeutic Radiology and Oncology (ESTRO) and the International Cardio-Oncology Society (IC-OS). *Eur Heart J* 2022;**43**:4229–361. https://doi.org/10.1093/eurheartj/ehac244
4. Rivero-Santana B, Saldana-Garcia J, Caro-Codon J, Zamora P, Moliner P, Martinez Monzonis A, *et al.* Anthracycline-induced cardiovascular toxicity: validation of the Heart Failure Association and International Cardio-Oncology Society risk score. *Eur Heart J* 2024;**46**:273–84. https://doi.org/10.1093/eurheartj/ehae496
5. Salz T, Zabor EC, de Nully Brown P, Dalton SO, Raghunathan NJ, Matasar MJ, *et al.* Preexisting cardiovascular risk and subsequent heart failure among non-Hodgkin lymphoma survivors. *J Clin Oncol* 2017;**35**:3837–43. https://doi.org/10.1200/JCO.2017.72.4211
6. Salloum FN, Tocchetti CG, Ameri P, Ardehali H, Asnani A, de Boer RA, *et al.* Priorities in cardio-oncology basic and translational science: GCOS 2023 symposium proceedings: JACC: CardioOncology state-of-the-art review. *JACC CardioOncol* 2023;**5**:715–31. https://doi.org/10.1016/j.jaccao.2023.08.003
7. Szmit S, Jurczak W, Zaucha JM, Drozd-Sokołowska J, Spychalowicz W, Joks M, *et al.* Pre-existing arterial hypertension as a risk factor for early left ventricular systolic dysfunction following (R)-CHOP chemotherapy in patients with lymphoma. *J Am Soc Hypertens* 2014;**8**:791–9. https://doi.org/10.1016/j.jash.2014.08.009

8. Moser EC, Noordijk EM, van Leeuwen FE, le Cessie S, Baars JW, Thomas J, *et al.* Long-term risk of cardiovascular disease after treatment for aggressive non-Hodgkin lymphoma. *Blood* 2006;**107**:2912–9. https://doi.org/10.1182/blood-2005-08-3392
9. Hershman DL, McBride RB, Eisenberger A, Tsai WY, Grann VR, Jacobson JS. Doxorubicin, cardiac risk factors, and cardiac toxicity in elderly patients with diffuse B-cell non-Hodgkin's lymphoma. *J Clin Oncol* 2008;**26**:3159–65. https://doi.org/10.1200/JCO.2007.14.1242
10. Tini G, Sarocchi M, Tocci G, Arboscello E, Ghigliotti G, Novo G, *et al.* Arterial hypertension in cancer: the elephant in the room. *Int J Cardiol* 2019;**281**:133–9. https://doi.org/10.1016/j.ijcard.2019.01.082
11. Kotwinski P, Smith G, Cooper J, Sanders J, Ma L, Teis A, *et al.* Body surface area and baseline blood pressure predict subclinical anthracycline cardiotoxicity in women treated for early breast cancer. *PLoS One* 2016;**11**:e0165262. https://doi.org/10.1371/journal.pone.0165262
12. Lyon AR, Dent S, Stanway S, Earl H, Brezden-Masley C, Cohen-Solal A, *et al.* Baseline cardiovascular risk assessment in cancer patients scheduled to receive cardiotoxic cancer therapies: a position statement and new risk assessment tools from the Cardio-Oncology Study Group of the Heart Failure Association of the European Society of Cardiology in collaboration with the International Cardio-Oncology Society. *Eur J Heart Fail* 2020;**22**:1945–60. https://doi.org/10.1002/ejhf.1920
13. Sharkey LC, Radin MJ, Heller L, Rogers LK, Tobias A, Matise I, *et al.* Differential cardiotoxicity in response to chronic doxorubicin treatment in male spontaneous hypertension-heart failure (SHHF), spontaneously hypertensive (SHR), and Wistar Kyoto (WKY) rats. *Toxicol Appl Pharmacol* 2013;**273**:47–57. https://doi.org/10.1016/j.taap.2013.08.012
14. Ayaon-Albarran A, Fernandez-Jimenez R, Silva-Guisasola J, Agüero J, Sanchez-Gonzalez J, Galan-Arriola C, *et al.* Systolic flow displacement using 3D magnetic resonance imaging in an experimental model of ascending aorta aneurysm: impact of rheological factors. *Eur J Cardiothorac Surg* 2016;**50**:685–92. https://doi.org/10.1093/ejcts/ezw132
15. Fernández-Jiménez R, Silva J, Martinez-Martinez S, López-Maderuelo MD, Nuno-Ayala M, García-Ruiz JM, *et al.* Impact of left ventricular hypertrophy on troponin release during acute myocardial infarction: new insights from a comprehensive translational study. *J Am Heart Assoc* 2015;**4**:e001218. https://doi.org/10.1161/JAHA.114.001218
16. García-Marqués F, Trevisan-Herraz M, Martínez-Martínez S, Camafeita E, Jorge I, Lopez JA, *et al.* A novel systems-biology algorithm for the analysis of coordinated protein responses using quantitative proteomics. *Mol Cell Proteomics* 2016;**15**:1740–60. https://doi.org/10.1074/mcp.M115.055905
17. Szklarczyk D, Gable AL, Lyon D, Junge A, Wyder S, Huerta-Cepas J, *et al.* STRING v11: protein-protein association networks with increased coverage, supporting functional discovery in genome-wide experimental datasets. *Nucleic Acids Res* 2019;**47**:D607–13. https://doi.org/10.1093/nar/gky1131
18. Galán-Arriola C, Lobo M, Vílchez-Tschischke JP, López GJ, de Molina-Iracheta A, Pérez-Martínez C, *et al.* Serial magnetic resonance imaging to identify early stages of anthracycline-induced cardiotoxicity. *J Am Coll Cardiol* 2019;**73**:779–91. https://doi.org/10.1016/j.jacc.2018.11.046
19. Melendez GC, Jordan JH, D'Agostino RB Jr, Lesnefsky EJ, Hundley WG. Accelerated left ventricular interstitial collagen deposition after receiving doxorubicin in hypertension. *J Am Coll Cardiol* 2018;**72**:1555–7. https://doi.org/10.1016/j.jacc.2018.07.028
20. Matsumura N, Zordoky BN, Robertson IM, Hamza SM, Parajuli N, Soltys CM, *et al.* Co-administration of resveratrol with doxorubicin in young mice attenuates detrimental late-occurring cardiovascular changes. *Cardiovasc Res* 2018;**114**:1350–9. https://doi.org/10.1093/cvr/cvy064
21. Kockskämper J, Pluteanu F. Left atrial myocardium in arterial hypertension. *Cells* 2022;**11**:3157. https://doi.org/10.3390/cells11193157
22. Davis RC, Hobbs FD, Kenkre JE, Roalfe AK, Hare R, Lancashire RJ, *et al.* Prevalence of left ventricular systolic dysfunction and heart failure in high risk patients: community based epidemiological study. *BMJ* 2002;**325**:1156. https://doi.org/10.1136/bmj.325.7373.1156
23. Nishikage T, Nakai H, Lang RM, Takeuchi M. Subclinical left ventricular longitudinal systolic dysfunction in hypertension with no evidence of heart failure. *Circ J* 2008;**72**:189–94. https://doi.org/10.1253/circj.72.189
24. Pun-García A, Clemente-Moragón A, Villena-Gutierrez R, Gómez M, Sanz-Rosa D, Díaz-Guerra A, *et al.* Beta-3 adrenergic receptor overexpression reverses aortic stenosis-induced heart failure and restores balanced mitochondrial dynamics. *Basic Res Cardiol* 2022;**117**:62. https://doi.org/10.1007/s00395-022-00966-z
25. Richards DA, Aronovitz MJ, Calamaras TD, Tam K, Martin GL, Liu P, *et al.* Distinct phenotypes induced by three degrees of transverse aortic constriction in mice. *Sci Rep* 2019;**9**:5844. https://doi.org/10.1038/s41598-019-42209-7
26. Guan D, Zhao Y, Zhang Y, Tang D, Wu Q. Proteomics analysis revealed an altered left ventricle protein profile in a mouse model of transverse aortic constriction. *Protein Pept Lett* 2016;**23**:125–31. https://doi.org/10.2174/0929866523666151125231747
27. Dai DF, Hsieh EJ, Chen T, Menendez LG, Basisty NB, Tsai L, *et al.* Global proteomics and pathway analysis of pressure-overload-induced heart failure and its attenuation by mitochondrial-targeted peptides. *Circ Heart Fail* 2013;**6**:1067–76. https://doi.org/10.1161/CIRCHEARTFAILURE.113.000406
28. Karamanlidis G, Bautista-Hernandez V, Fynn-Thompson F, Del Nido P, Tian R. Impaired mitochondrial biogenesis precedes heart failure in right ventricular hypertrophy in congenital heart disease. *Circ Heart Fail* 2011;**4**:707–13. https://doi.org/10.1161/CIRCHEARTFAILURE.111.961474
29. Neubauer S. The failing heart–an engine out of fuel. *N Engl J Med* 2007;**356**:1140–51. https://doi.org/10.1056/NEJMra063052
30. Esposito A, De Cobelli F, Perseghin G, Pieroni M, Belloni E, Mellone R, *et al.* Impaired left ventricular energy metabolism in patients with hypertrophic cardiomyopathy is related to the extension of fibrosis at delayed gadolinium-enhanced magnetic resonance imaging. *Heart* 2009;**95**:228–33. https://doi.org/10.1136/hrt.2008.142562
31. Heyne JP, Rzanny R, Hansch A, Leder U, Reichenbach JR, Kaiser WA. 31P-MR spectroscopic imaging in hypertensive heart disease. *Eur Radiol* 2006;**16**:1796–802. https://doi.org/10.1007/s00330-006-0170-0
32. Smith CS, Bottomley PA, Schulman SP, Gerstenblith G, Weiss RG. Altered creatine kinase adenosine triphosphate kinetics in failing hypertrophied human myocardium. *Circulation* 2006;**114**:1151–8. https://doi.org/10.1161/CIRCULATIONAHA.106.613646
33. Abraham MR, Bottomley PA, Dimaano VL, Pinheiro A, Steinberg A, Traill TA, *et al.* Creatine kinase adenosine triphosphate and phosphocreatine energy supply in a single kindred of patients with hypertrophic cardiomyopathy. *Am J Cardiol* 2013;**112**:861–6. https://doi.org/10.1016/j.amjcard.2013.05.017
34. Macnaught G, Oikonomidou O, Rodgers CT, Clarke W, Cooper A, McVicars H, *et al.* Cardiac energetics before, during, and after anthracycline-based chemotherapy in breast cancer patients using (31)P magnetic resonance spectroscopy: a pilot study. *Front Cardiovasc Med* 2021;**8**:653648. https://doi.org/10.3389/fcvm.2021.653648
35. Gupta A, Rohlfsen C, Leppo MK, Chacko VP, Wang Y, Steenbergen C, *et al.* Creatine kinase-overexpression improves myocardial energetics, contractile dysfunction and survival in murine doxorubicin cardiotoxicity. *PLoS One* 2013;**8**:e74675. https://doi.org/10.1371/journal.pone.0074675
36. Maslov MY, Chacko VP, Hirsch GA, Akki A, Leppo MK, Steenbergen C, *et al.* Reduced in vivo high-energy phosphates precede Adriamycin-induced cardiac dysfunction. *Am J Physiol Heart Circ Physiol* 2010;**299**:H332–7. https://doi.org/10.1152/ajpheart.00727.2009
37. Monga S, Valkovič L, Myerson SG, Neubauer S, Mahmod M, Rider OJ. Role of cardiac energetics in aortic stenosis disease progression: identifying the high-risk metabolic phenotype. *Circ Cardiovasc Imaging* 2023;**16**:e014863. https://doi.org/10.1161/CIRCIMAGING.122.014863
38. Díaz-Guerra A, Villena-Gutiérrez R, Clemente-Moragón A, Gómez M, Oliver E, Fernández-Tocino M, *et al.* Anthracycline cardiotoxicity induces progressive changes in myocardial metabolism and mitochondrial quality control: novel therapeutic target. *JACC CardioOncol* 2024;**6**:217–32. https://doi.org/10.1016/j.jaccao.2024.02.005
39. Ferdinandy P, Baczkó I, Bencsik P, Giricz Z, Görbe A, Pacher P, *et al.* Definition of hidden drug cardiotoxicity: paradigm change in cardiac safety testing and its clinical implications. *Eur Heart J* 2019;**40**:1771–7. https://doi.org/10.1093/eurheartj/ehy365
40. Garcia-Pavia P, Kim Y, Restrepo-Cordoba MA, Lunde IG, Wakimoto H, Smith AM, *et al.* Genetic variants associated with cancer therapy-induced cardiomyopathy. *Circulation* 2019;**140**:31–41. https://doi.org/10.1161/CIRCULATIONAHA.118.037934
41. Ibáñez B, Gomes-Silva M. Remote ischemic conditioning for anthracycline cardiotoxicity: the need to protect the most vulnerable. *JACC CardioOncol* 2023;**5**:356–9. https://doi.org/10.1016/j.jaccao.2023.05.002
42. Landoni G, Zangrillo A, Lomivorotov VV, Likhvantsev V, Ma J, De Simone F, *et al.* Cardiac protection with phosphocreatine: a meta-analysis. *Interact Cardiovasc Thorac Surg* 2016;**23**:637–46. https://doi.org/10.1093/icvts/ivw171
43. Sharma S, Merghani A, Mont L. Exercise and the heart: the good, the bad, and the ugly. *Eur Heart J* 2015;**36**:1445–53. https://doi.org/10.1093/eurheartj/ehv090
44. Foulkes SJ, Howden EJ, Haykowsky MJ, Antill Y, Salim A, Nightingale SS, *et al.* Exercise for the prevention of anthracycline-induced functional disability and cardiac dysfunction: the BREXIT study. *Circulation* 2023;**147**:532–45. https://doi.org/10.1161/CIRCULATIONAHA.122.062814
45. Shah SJ, Rigolli M, Javidialsaadi A, Patel RB, Khadra S, Goyal P, *et al.* Cardiac myosin inhibition in heart failure with normal and supranormal ejection fraction: primary results of the EMBARK-HFpEF trial. *JAMA Cardiol* 2024;**10**:170. https://doi.org/10.1001/jamacardio.2024.3810
46. Saberi S, Cardim N, Yamani M, Schulz-Menger J, Li W, Florea V, *et al.* Mavacamten favorably impacts cardiac structure in obstructive hypertrophic cardiomyopathy: EXPLORER-HCM cardiac magnetic resonance substudy analysis. *Circulation* 2021;**143**:606–8. https://doi.org/10.1161/CIRCULATIONAHA.120.052359
47. Perez-Riverol Y, Bai J, Bandla C, García-Seisdedos D, Hewapathirana S, Kamatchinathan S, *et al.* The PRIDE database resources in 2022: a hub for mass spectrometry-based proteomics evidences. *Nucleic Acids Res* 2022;**50**:D543–52. https://doi.org/10.1093/nar/gkab1038